Composites Communications 29 (2022) 101025

Contents lists available at ScienceDirect

Composites Communications

journal homepage: www.elsevier.com/locate/coco

Nanocomposite block copolymer membranes with enhanced permeance and robustness by carbon nanotube doping

Qianqian Lan [a], Nina Yan [b,**], Hao Yang [c], Yong Wang [d,*]

[a] The Key Laboratory of Synthetic and Biological Colloids, Ministry of Education, School of Chemical and Material Engineering, International Joint Research Laboratory for Nano Energy Composites, Jiangnan University, Wuxi, 214122, Jiangsu, PR China
[b] Institute of Agricultural Facilities and Equipment, Jiangsu Academy of Agricultural Sciences, Key Laboratory for Protected Agricultural Engineering in the Middle and Lower Reaches of Yangtze River, Ministry of Agriculture and Rural Affairs, Nanjing, 210014, Jiangsu, PR China
[c] College of Chemistry & Chemical Engineering, Yantai University, Yantai, 264005, Shandong, PR China
[d] State Key Laboratory of Materials-Oriented Chemical Engineering, College of Chemical Engineering, Nanjing Tech University, Nanjing, 211816, Jiangsu, PR China

ARTICLE INFO

Keywords:
Block copolymer
Carbon nanotube
Nanocomposite membrane
Selective swelling

ABSTRACT

Block copolymers (BCPs) have received extensive attention in the preparation of advanced membranes for precise separations. However, BCP-derived membranes usually suffer from insufficient mechanical robustness, especially for the most extensively studied polystyrene-based ones. Herein, carbon nanotubes (CNTs) are incorporated into polystyrene-*block*-poly (2-vinyl pyridine) (S2VP) membranes to enhance the mechanical robustness and water permeance. It is found that mild oxidation is enough to enable the homogeneous dispersion of CNTs in the S2VP solution. The CNT/S2VP mixture is directly coated on macroporous substrates, followed by selective swelling-induced pore generation to produce the CNT-doped S2VP nanocomposite membranes. The as-prepared membranes are featured with two sets of pores: swelling-induced pores and incompatibility-induced nanoscale gaps between CNTs and the S2VP matrix, leading to improved permeances without any decrease of the retention performances. Also, owing to the presence of CNTs in the polymer matrix, the membranes show excellent mechanical robustness and exhibit better pressure resistance than neat S2VP membrane without CNT doping. This work demonstrates a simple yet efficient strategy to prepare BCP-based nanocomposite membranes with enhanced permeance and robustness at no expense of retention.

1. Introduction

Block copolymers (BCPs) are receiving growing interest in preparing high-resolution separation membranes because of their unique microphase separation property leading to well-ordered nanostructures [1–3]. Extensive works have been focused on the preparation of BCP-derived separation membranes and their potential applications in water treatment, bioengineering, hemodialysis, and batteries [4–7]. The amphiphilic BCPs can be easily cavitated to form nanoporous structures with relatively uniform pore sizes in the range of 10–100 nm following the mechanism of selective swelling-induced pore generation [8,9]. This is highly desirable for the facile and controllable preparation of high-performance separation membranes.

BCPs are usually employed as the selective layers composited on the supporting macroporous substrates [10]. Most BCP membranes currently investigated are derived from polystyrene (PS)-based BCPs because they are available with nearly arbitrary block ratios with very narrow molecular weight distributions. Unfortunately, PS as an amorphous polymer with a glass transition temperature of ~ 100 °C suffer from poor mechanical robustness [11]. Several methodologies have been proposed to enhance the mechanical robustness of PS-containing BCP membranes. For example, introducing a rubbery third component into the PS-containing BCPs has been proved as an effective way, including physically blending a rubbery polymer [12] and grafting a rubbery third block [13,14]. It is also valid to replace the PS domain in BCPs with a stronger one, such as polysulfone (PSF) [15,16]. Nevertheless, although inorganic nanofillers have been extensively used to improve the mechanical stability of a large variety of polymeric materials including separation membranes, there is no reports on the use of inorganic nanofillers to enhance the mechanical strength of BCP

* Corresponding author.
** Corresponding author.
E-mail addresses: yannina@jaas.ac.cn (N. Yan), yongwang@njtech.edu.cn (Y. Wang).

https://doi.org/10.1016/j.coco.2021.101025
Received 18 November 2021; Received in revised form 4 December 2021; Accepted 5 December 2021
Available online 8 December 2021

membranes prepared by selective swelling.

Carbon nanotubes (CNTs) have been applied as an impressive inorganic nanofillers or dopants in various membranes for ultrafiltration, nanofiltration, and reverse osmosis as they can regulate the structures and physicochemical properties of the target membranes [17–20]. For example, Lee et al. incorporated oxidized CNTs into PSF matrix to prepare CNT/PSF nanocomposite membranes with improved porosity mainly due to the incompatibility induced pore formation between CNTs and PSF [21]. More importantly, doping with CNTs can greatly enhance the mechanical stabilities of PSF membranes and polyamide membranes thanks to the extraordinary mechanical strength of CNTs [22–25]. Inspired by the strong enhancement effect of CNTs in polymer matrix, we expect that doping with CNTs would be a useful approach to prepare PS-containing BCP membranes with high porosity and improved robustness. Moreover, CNTs can be arrested by BCPs via strong π-π interactions between CNTs and PS blocks, leading to excellent dispersity and anchoring of the doped CNTs to ensure good modification effect. However, current works on CNT/BCP nanocomposite membranes are mainly focused on the uniform dispersion of CNTs with the assistance of BCPs [26]. That is, BCPs work as a dispersant rather than the matrix. Therefore, insights into the effect of the doped CNTs on BCP porous matrixes have not been explored, but are highly desired for the sake of development of highly permeable but strong membranes.

In this work, CNTs are mildly oxidized, and then doped into polystyrene-*block*-poly (2-vinyl pyridine) (PS-*b*-P2VP, denoted as S2VP) membranes for enhancing water permeance and robustness. The CNT/S2VP solution is directly coated on macroporous polyvinylidene fluoride (PVDF) substrates, and the coated CNT/S2VP layers are simply cavitated by the process of selective swelling-induced pore generation (Fig. 1). The obtained CNT-doped S2VP nanocomposite membranes exhibit synergistically improved water permeance and mechanical robustness.

2. Results and discussion

2.1. Mild oxidization of CNTs

As CNTs have strong intertube interactions, the dispersion of the CNTs in the S2VP solution is a major concern for obtaining a homogeneous CNT/S2VP solution for the preparation of integrate, uniform and thin membranes [26,27]. It has been reported that BCPs are potential for improving the dispersion of CNTs [28]. However, we found that the pristine CNTs (*p*-CNTs) have quite poor dispersion in the S2VP solution. Therefore, to enhance the dispersion of CNTs, surface functionalization is required.

Among various functionalization methods, acid oxidation has been regarded as an efficient one because the oxidation degrees can be simply tuned by changing the reaction conditions, such as temperature, time, and the volume ratio of the acid and the CNTs [17]. Here, we chose to oxidize CNTs in the mixture of HNO_3 and H_2SO_4 at 50 °C. The schematic diagram for the mild oxidation of CNTs is illustrated in Fig. 2a. After oxidation, some carboxylic groups are generated on the surface of CNTs. The presence of carboxylic groups disrupts the long range π conjugation of CNTs, leading to the improved dispersion of CNTs [29]. As shown in Fig. 2b, the *p*-CNTs are precipitated in the S2VP solution even after strong sonication. After oxidation, the dispersion of the oxidized CNTs (*o*-CNTs) in the S2VP solution is significantly improved, which has been evidenced by the homogeneous solution without any macroscopic aggregations (Fig. 2c). The FT-IR spectra of the *p*-CNTs and *o*-CNTs are given in Fig. 2d. A weak peak centering around 1720 cm^{-1} corresponded to the C═O stretching of carboxylic groups is observed, confirming the mild oxidation of the *p*-CNTs [30]. Note that the mild oxidation has less negative impact on the mechanical strength of CNTs. Importantly, the *o*-CNTs maintain hydrophobicity [31] owing to the low degree of oxidation under the quite low oxidation temperature during mild oxidation (Fig. S1). This is essential for the dispersion of the *o*-CNTs in the hydrophobic organic solvent used to dissolve BCPs.

2.2. Morphologies of CNT-doped S2VP nanocomposite membranes

By using the homogeneous CNT/S2VP solutions with varied *o*-CNTs contents, we prepared a series of CNT-doped S2VP nanocomposite membranes. The obtained membranes were denoted as S2VP-X, where X is the mass ratio of CNTs and S2VP. We first investigated the surface morphologies of the membranes. The S2VP-0 membrane (neat S2VP membrane without doping of CNTs) is nonporous with a smooth surface before swelling (Fig. 3a). After CNTs doping, the S2VP-0.1 membrane maintains nonporous but exhibits rich bright dots on the surface ascribed to the *o*-CNTs with good conductivity, confirming the crosswise uniform distribution of the doped *o*-CNTs in the S2VP matrix (Fig. 3b). After soaking the nanocomposite membranes in ethanol at 65 °C for 1 h, the nonporous CNT/S2VP layers turned to be porous following the mechanism of selective swelling-induced pore generation. As shown in Fig. 3c–d and Fig. S2, all the membranes exhibit porous surface structures with many round nanopores. Meanwhile, the S2VP-0 membrane shows a rough surface with micellized S2VP, which is indicative of the high swelling degree. By contrast, the surface of the CNT-doped S2VP nanocomposite membrane is relatively smooth without micellization. This is because some S2VP molecules are involved in encapsulating *o*-

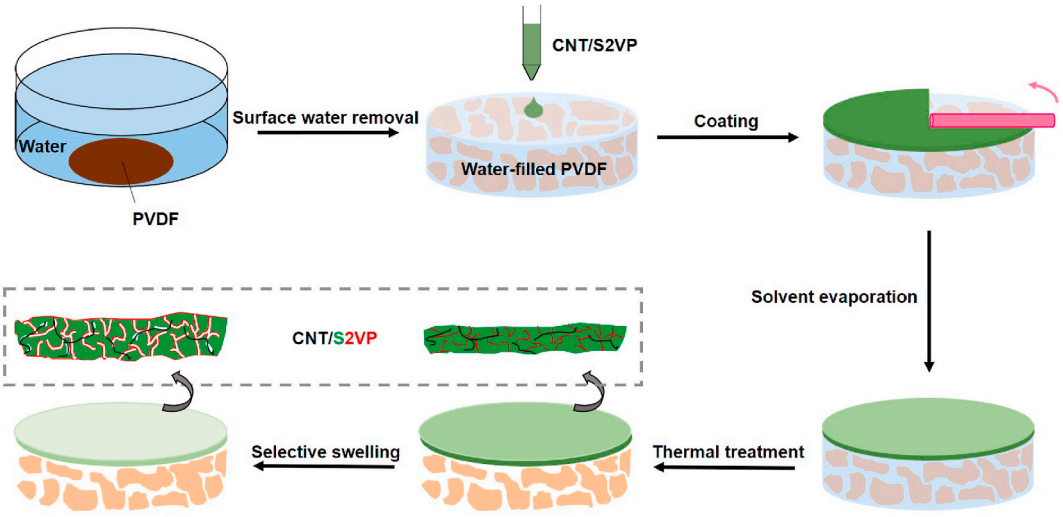

Fig. 1. The schematic diagram for the preparation of CNT-doped S2VP nanocomposite membranes.

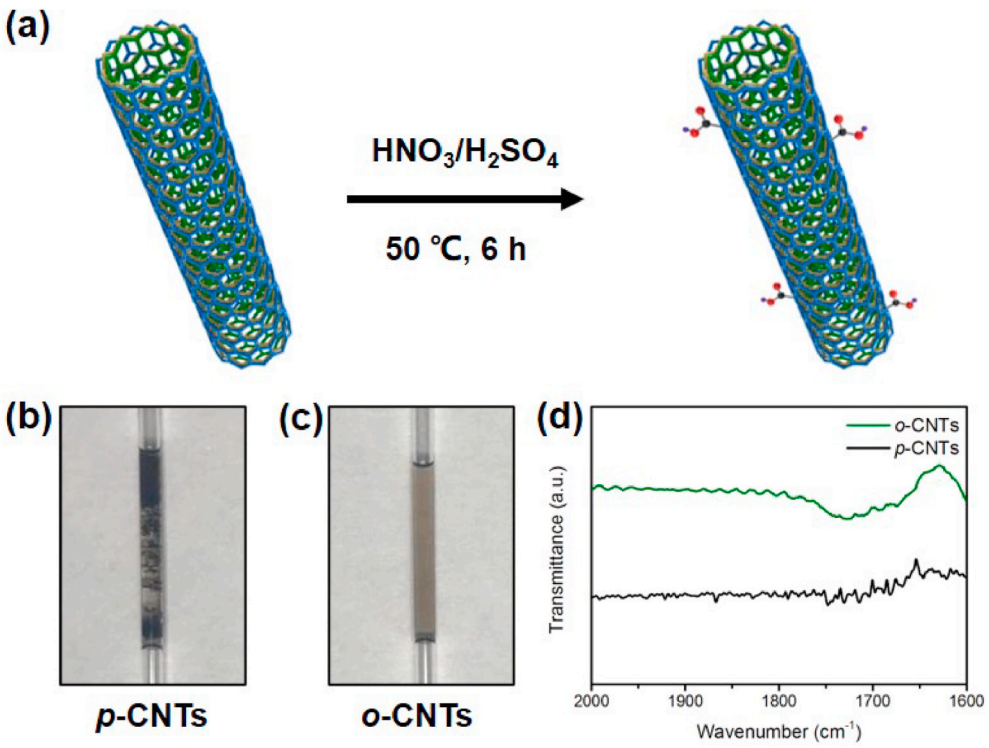

Fig. 2. The mild oxidization of CNTs. (a) The schematic diagram of the mild oxidization of *p*-CNTs. Photographs of (b) the *p*-CNTs and (c) the *o*-CNTs dispersed in the S2VP solution with the CNT/S2VP mass ratio of 0.05. The mixtures were filled into capillary tubes for better observation. (d) FT-IR spectra of the *p*-CNTs and *o*-CNTs.

CNTs by anchoring PS blocks on tube walls, leading to slightly repressed swelling degree [32]. Moreover, compared with the neat S2VP membrane, the CNT-doped S2VP nanocomposite membrane exhibits higher porosity contributing from the incompatible gaps [33] between the dispersed *o*-CNTs and S2VP matrix (Fig. 3e–f). It should be noted that this incompatibility occurs to a limited degree, thus leading to nanoscale gaps rather than large-sized defects.

We then examined the cross-sectional morphologies of the membranes. As shown in Fig. 3g, the nonporous CNT/S2VP layer is closely jointed with the support, verifying the strong adhesion between the two layers after thermal treatment. The CNT/S2VP layers with varied *o*-CNTs contents share a similar thickness of ~ 1.3 μm (Fig. S3). After selective swelling, highly porous CNT/S2VP layers with bi-continuous structures can be observed in all membranes, and the porous CNT/S2VP layers are still jointed tightly with the supports (Fig. 3h and Fig. S4). The thickness of the porous CNT/S2VP layers is increased to ~ 2.2 μm. According to the changes of the thicknesses before and after selective swelling, the porosity of the CNT/S2VP layers is estimated to be ~ 41%. Moreover, dispersed *o*-CNTs can be clearly observed in the cross section depicted in Fig. 3i, indicating the uniformly dispersion of the *o*-CNTs inside the membrane, which agrees with the surface SEM observations discussed above. These results indicate the good dispersity of the *o*-CNTs during the whole membrane preparation process including solvent evaporation and selective swelling mainly due to the strong interactions between CNTs and PS blocks. Accordingly, the incompatibility-induced gaps also exist inside the membrane although they can hardly be distinguished from the swelling-induced pores in cross section.

2.3. Separation performances of CNT-doped S2VP nanocomposite membranes

We first examined the water permeances of the CNT-doped S2VP nanocomposite membranes with varied CNT/S2VP mass ratios of 0–0.05. Prior to swelling, the membranes produced no water permeation under the pressure of 0.2 bar, confirming their nonporous structure after thermal treatment. After swelling in ethanol at 65 °C for 1 h, the water permeances of the membranes are given in Fig. 4a. The S2VP-0 membrane shows a permeance of 1156 $L{\cdot}m^{-2}{\cdot}h^{-1}{\cdot}bar^{-1}$. After doping with the *o*-CNTs, all the membranes exhibit higher permeances than the S2VP-0 membrane. For example, the permeance of the S2VP-0.005 membrane is 1204 $L{\cdot}m^{-2}{\cdot}h^{-1}{\cdot}bar^{-1}$, which is increased to 1643 $L{\cdot}m^{-2}{\cdot}h^{-1}{\cdot}bar^{-1}$ for the S2VP-0.01 membrane. With further increase in the CNT/S2VP mass ratio, the S2VP-0.03 membrane and the S2VP-0.05 membrane show permeances of 1485 $L{\cdot}m^{-2}{\cdot}h^{-1}{\cdot}bar^{-1}$ and 1258 $L{\cdot}m^{-2}{\cdot}h^{-1}{\cdot}bar^{-1}$, respectively. That is, compared with the S2VP-0 membrane, the increments in the permeance of the CNT-doped S2VP nanocomposite membranes are 4.2%, 42.2%, 28.5%, and 8.8%, respectively. The improved permeance of the CNT-doped S2VP nanocomposite membranes than the S2VP-0 membrane is mainly because the gaps between the *o*-CNTs and the S2VP matrix create extra water permeation pathways. The inner tubes of CNTs play an ignorable role on water permeance because the inner diameter of CNTs is much smaller than the size of pores and gaps and the doping amount of CNTs is tiny. However, the permeances are increased at reduced amplitude in the cases of the membranes with higher CNT/S2VP mass ratios, which is mainly because the hydrophobicity of *o*-CNTs increases the mass transfer resistance and thus hinders the water permeation inside the membranes.

Further, we examined the retention properties of the CNT-doped S2VP nanocomposite membranes by measuring the rejection rates of the membranes to bovine serum albumin (BSA) and SiO_2 nanoparticles. As shown in Fig. 4b, all the membranes show similar retention properties regardless of the doping amount of the *o*-CNTs. The rejection rates to BSA and SiO_2 nanoparticles maintain ~ 5% and ~ 80%, respectively. These results illustrate that doping of the *o*-CNTs nearly has no influence on the rejection performance of the membranes. Note that the hydrophobic *o*-CNTs are decorated with amphiphilic S2VP molecules, and S2VP membranes are hydrophilic according to the selective swelling mechanism. Besides, the BSA in the feed solution is nearly equal to the summary of BSA in the rejection and the retention solutions during the

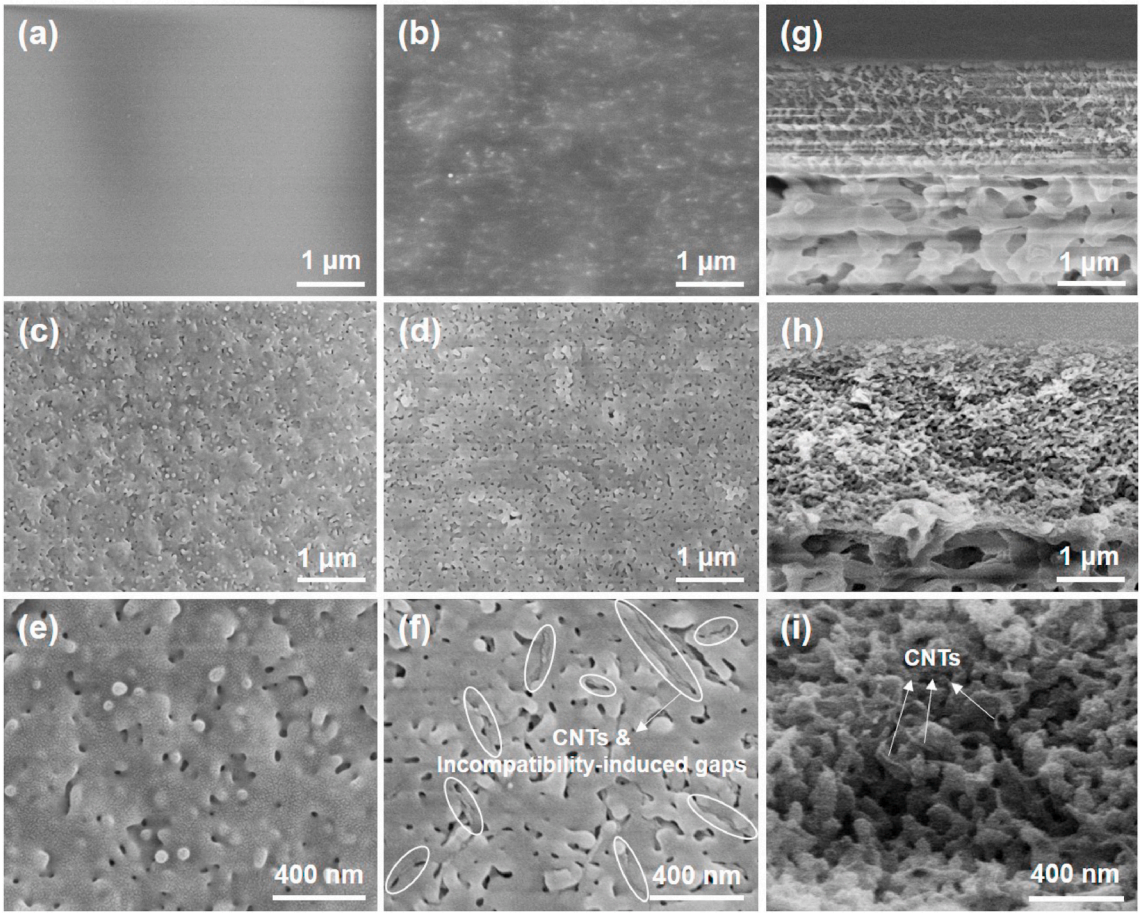

Fig. 3. Morphologies of CNT-doped S2VP nanocomposite membranes. Surface SEM images of (a) the S2VP-0 membrane and (b) the S2VP-0.1 membrane before selective swelling. Surface SEM images of (c, e) the S2VP-0 membrane and (d, f) the S2VP-0.05 membrane after selective swelling. Cross-sectional SEM images of the S2VP-0.03 membrane (g) before and (h, i) after selective swelling. The *o*-CNTs and the incompatibility-induced gaps between *o*-CNTs and S2VP matrix are highlighted in (f).

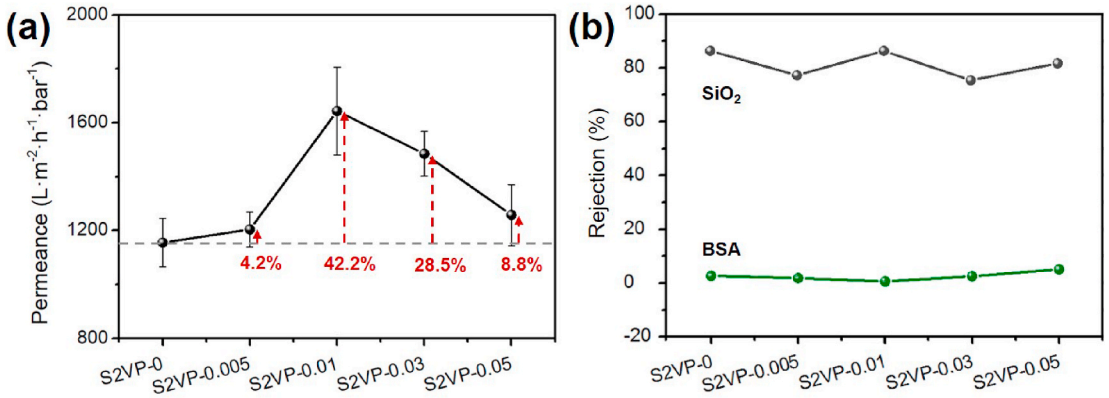

Fig. 4. Separation performances of CNT-doped S2VP nanocomposite membranes. (a) Water permeance, (b) rejection rates to BSA and SiO_2 nanoparticles of the CNT-doped S2VP nanocomposite membranes.

rejection experiments. There results suggest a low protein adsorption and good anti-fouling property of the membranes. Moreover, the permeance maintains unchanged during the test. Therefore, membranes possess a good stability of the separation performance. The size-sieving effect is dominant in the rejection of the solutes. The hydrated diameter of BSA molecules is ~ 6 nm while the diameter of the SiO_2 nanoparticles is in the range of 5–10 nm [34]. Moreover, BSA molecules are in the shape of flexible ellipsoid with the size of 4.0 × 4.0 × 14.0 nm^3, while the SiO_2 nanoparticles are sphere-shaped and rigid [35]. Therefore, the membranes exhibit low rejection rates to BSA while high rejection rates to SiO_2 nanoparticles due to the different sizes, shapes, and deformabilities of BSA molecules and SiO_2 nanoparticles [36]. Moreover, compared with other CNT-doped membranes reported in literature, the CNT-doped S2VP nanocomposite membranes can achieve higher permeance with a comparable rejection property (Table S1), indicating the superiority of the membranes prepared by the CNT doping-selective

swelling strategy.

2.4. Pressure resistance of CNT-doped S2VP nanocomposite membranes

To evaluate the mechanical robustness of the CNT-doped S2VP nanocomposite membranes, we investigated the pressure resistance of the membranes by measuring the water fluxes under elevated transmembrane pressures (TMPs). In general, the water flux is linearly increased with the increased TMPs if the porous membrane is robust to withstand compaction [37]. The water flux of the S2VP-0 membrane maintains almost unchanged when the TMP is higher than 0.8 bar (Fig. 5a), indicating the severe compaction of the membrane without doping of the *o*-CNTs as a result of the soft nature of S2VP and the highly porous structure of the swelling-treated S2VP membranes. By contrast, the CNT-doped S2VP nanocomposite membranes can withstand the TMP elevated to 1.0 bar, demonstrating their improved pressure resistance benefiting from the mechanical reinforcement effect of *o*-CNTs. Besides, the nonlinearly increased water flux indicates a decreased stability of the membranes at high TMPs due to the poor mechanical robustness of the amorphous PS.

To further reveal the influence of the *o*-CNTs contents on the pressure resistance of the membranes, we calculated the increments in water fluxes of the membranes under the TMP ranging from 0.2 bar to 0.6 bar. The increment in water fluxes of the S2VP-0 membrane is 85%, which is increased to 140%, 148%, 119%, and 114% for the S2VP-0.005, S2VP-0.01, S2VP-0.03, and S2VP-0.05 membranes, respectively (Fig. 5b). The increased increments in water fluxes suggest the enhanced pressure resistance of the CNT-doped S2VP nanocomposite membranes. Particularly, the S2VP-0.005 and S2VP-0.01 membranes hold dramatic increments in water fluxes, which is indicative of their superior pressure-resisting properties. That is, doping with *o*-CNTs at the CNT/S2VP mass ratio lower than 0.01 is favorable to enhance the mechanical robustness of the S2VP membranes. However, higher CNT/S2VP mass ratios lead to more gaps between the *o*-CNTs and the S2VP matrix, which degrades the mechanical strength of the membranes. Overall, the S2VP-0.01 membrane is optimal to enable both high water permeance and good mechanical robustness.

In addition, the porous structures can influence the mechanical robustness of the membranes. To demonstrate this, we immersed the S2VP-0.01 membrane in ethanol at different temperatures to alter the swelling degree for regulating porous structures. As shown in Fig. 5c, the water fluxes of the membranes prepared by swelling at 60 °C and 65 °C are increased under the TMPs ranging from 0.2 bar to 1.0 bar, and then keep nearly unchanged under higher TMPs due to the completely structural compaction. By contrast, the membrane prepared by swelling at 55 °C exhibits gradually increased water fluxes under the TMPs of 0.2–1.5 bar, which is indicative of stronger pressure resistance. As shown in Fig. 5d–e, the 55 °C-treated membrane exhibits lower swelling degree with smaller pores than the 65 °C-treated membrane. That is, the pressure resistance relies on the porous structures of the membranes. Therefore, the mechanical robustness can be further improved by regulating the porous structures of the membranes.

3. Conclusion

In this work, we report a CNT doping strategy to simultaneously improve the water permeance and mechanical robustness of BCP membranes. CNTs can be homogeneously dispersed in S2VP solutions after a simple and mild oxidation treatment. The CNT-doped S2VP nanocomposite membranes are prepared by coating the CNT/S2VP solutions on the macroporous substrates, followed by solvent evaporation, thermal treatment, and selective swelling. Many incompatibility-induced nanoscale gaps are formed between the CNTs and the S2VP matrix, leading to improved water permeance of the membranes. Thanks to the strong mechanical strength of CNTs, the CNT-doped S2VP nanocomposite membranes achieve enhanced robustness against

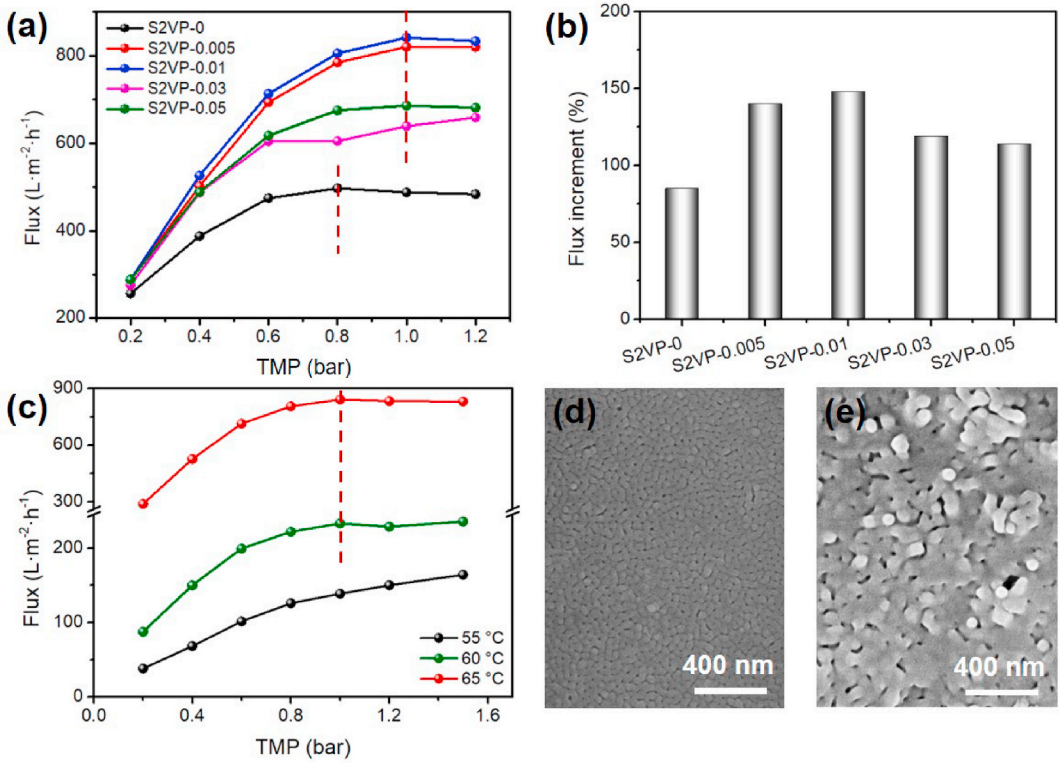

Fig. 5. Pressure resistance of CNT-doped S2VP nanocomposite membranes. (a) The change of water fluxes with the TMPs and (b) the increments in water fluxes under the TMP ranging from 0.2 bar to 0.6 bar for the membranes with different CNT/S2VP mass ratios. (c) The change of water fluxes with the TMPs for the S2VP-0.01 membrane after selective swelling at different temperatures. Surface SEM images of the S2VP-0.01 membrane after selective swelling at (d) 55 °C and (e) 65 °C.

pressure. This work demonstrates the great potential of CNT doping in upgrading the mechanical stability of BCP membranes at no expense of their separation performances.

CRediT authorship contribution statement

Qianqian Lan: Software, Writing – review & editing, Visualization, Funding acquisition. **Nina Yan:** Conceptualization, Software, Writing – original draft, Funding acquisition. **Hao Yang:** Methodology, Investigation, Writing – original draft. **Yong Wang:** Resources, Supervision, Project administration.

Declaration of competing interest

The authors declare that they have no known competing financial interests or personal relationships that could have appeared to influence the work reported in this paper.

Acknowledgements

Financial support from the National Natural Science Foundation of China (22008086), the China Postdoctoral Science Foundation (2020M671332), the Jiangsu Postdoctoral Science Foundation (2020Z210), and the Jiangsu Provincial Key Research and Development Project (BE2020307) is gratefully acknowledged.

Appendix A. Supplementary data

Supplementary data to this article can be found online at https://doi.org/10.1016/j.coco.2021.101025.

References

[1] D.L. Zhong, J.M. Zhou, Y. Wang, Hollow-fiber membranes of block copolymers by melt spinning and selective swelling, J. Membr. Sci. 632 (2021) 119374.
[2] M.M. Rahman, Selective swelling and functionalization of integral asymmetric isoporous block copolymer membranes, Macromol. Rapid Commun. 42 (2021) 2100235.
[3] H. Ahn, S. Park, S.W. Kim, P.J. Yoo, D.Y. Ryu, T.P. Russell, Nanoporous block copolymer membranes for ultrafiltration: a simple approach to size tunability, ACS Nano 8 (2014) 11745–11752.
[4] M. Radjabian, V. Abetz, Advanced porous polymer membranes from self-assembling block copolymers, Prog. Polym. Sci. 102 (2020) 101219.
[5] H.Z. Yu, X.Y. Qiu, N. Moreno, Z.W. Ma, V.M. Calo, S.P. Nunes, K.V. Peinemann, Self-assembled asymmetric block copolymer membranes: bridging the gap from ultra- to nanofiltration, Angew. Chem. Int. Ed. 54 (2015) 13937–13941.
[6] D.L. Zhong, Z.G. Wang, J.M. Zhou, Y. Wang, Additive-free preparation of hemodialysis membranes from block copolymers of polysulfone and polyethylene glycol, J. Membr. Sci. 618 (2021) 118690.
[7] H. Yang, X.S. Shi, S.Y. Chu, Z.P. Shao, Y. Wang, Design of block-copolymer nanoporous membranes for robust and safer lithium-ion battery separators, Advanced Science 8 (2021) 2003096.
[8] Z.G. Wang, X.P. Yao, Y. Wang, Swelling-induced mesoporous block copolymer membranes with intrinsically active surfaces for size-selective separation, J. Mater. Chem. 22 (2012) 20542–20548.
[9] Y. Wang, F. Li, An emerging pore-making strategy: confined swelling-induced pore generation in block copolymer materials, Adv. Mater. 23 (2011) 2134–2148.
[10] J.M. Zhou, Y. Wang, Selective swelling of block copolymers: an upscalable greener process to ultrafiltration membranes? Macromolecules 53 (2020) 5–17.
[11] J.E. Mark, Physical Properties of Polymers Handbook, second ed., Springer Science, New York, 2007.
[12] Z.G. Wang, R. Liu, Q.Q. Lan, Y. Wang, Selective swelling blends of block copolymers for nanoporous membranes with enhanced permeability and robustness, J. Polym. Sci. B Polym. Phys. 55 (2017) 1617–1625.
[13] A. Jung, V. Filiz, S. Rangou, K. Buhr, P. Merten, J. Hahn, J. Clodt, C. Abetz, V. Abetz, Formation of integral asymmetric membranes of AB diblock and ABC triblock copolymers by phase inversion, Macromol. Rapid Commun. 34 (2013) 610–615.
[14] Z.G. Wang, Y. Wang, Highly permeable and robust responsive nanoporous membranes by selective swelling of triblock terpolymers with a rubbery block, Macromolecules 49 (2016) 182–191.
[15] Z.G. Wang, R. Liu, H. Yang, Y. Wang, Nanoporous polysulfones with in situ PEGylated surfaces by a simple swelling strategy using paired solvents, Chem. Commun. 53 (2017) 9105–9108.
[16] H. Yang, J.M. Zhou, Z.G. Wang, X.S. Shi, Y. Wang, Selective swelling of polysulfone/poly(ethylene glycol) block copolymer towards fouling-resistant ultrafiltration membranes, Chin. J. Chem. Eng. 28 (2020) 98–103.
[17] R.Q. Wang, D.H. Chen, Q. Wang, Y.B. Ying, W.L. Gao, L.J. Xie, Recent advances in applications of carbon nanotubes for desalination: a review, Nanomaterials 10 (2020) 1203.
[18] H.Y. Zhao, S. Qiu, L.G. Wu, L. Zhang, H.L. Chen, C.J. Gao, Improving the performance of polyamide reverse osmosis membrane by incorporation of modified multi-walled carbon nanotubes, J. Membr. Sci. 450 (2014) 249–256.
[19] P. Yang, B. Zhang, H. Wu, L. Cao, X. He, Z. Jiang, Imidazolium-functionalized carbon nanotubes crosslinked with imidazole poly(ether ether ketone) for fabricating anion exchange membranes with high hydroxide conductivity and dimension stability, Electrochim. Acta 318 (2019) 572–580.
[20] Y. Wang, J. Duan, X. Du, X. Liang, B. Liu, Z. Sun, Y. Men, W. Hu, G. Zhu, High performance of polyethylene composite separators modified by carbon nanotube, lithium salt and SiO_2 nanoparticles for lithium ion batteries, Composites Communications 28 (2021) 100976.
[21] T.H. Lee, M.Y. Lee, H.D. Lee, J.S. Roh, H.W. Kim, H.B. Park, Highly porous carbon nanotube/polysulfone nanocomposite supports for high-flux polyamide reverse osmosis membranes, J. Membr. Sci. 539 (2017) 441–450.
[22] Y.Y. Tang, H.Y. Yu, Y.L. Xing, C.J. Gao, J. Xu, Microstructure and desalination performance of polyamide membranes interfacially regulated via single-side post-modified CNTs networks, Desalination 482 (2020) 114408.
[23] S. Singh, A.M. Varghese, K.S.K. Reddy, G.E. Romanos, G.N. Karanikolos, Polysulfone mixed-matrix membranes comprising poly(ethylene glycol)-grafted carbon nanotubes: mechanical properties and CO_2 separation performance, Ind. Eng. Chem. Res. 60 (2021) 11289–11308.
[24] X. Zhang, W. Li, Z. Zhao, Y. He, P. Dong, Y. Ma, J. Huang, A theoretical model for the tensile modulus of polymer/CNT nanocomposites over a wide temperature range, Composites Communications 28 (2021) 100971.
[25] J. Zeng, W. Ma, Q. Wang, S. Yu, M.T. Innocent, H. Xiang, M. Zhu, Strong, high stretchable and ultrasensitive SEBS/CNTs hybrid fiber for high-performance strain sensor, Composites Communications 25 (2021) 100735.
[26] X.P. Yao, J. Li, Z.G. Wang, L. Kong, Y. Wang, Highly permeable and robust membranes assembled from block-copolymer-functionalized carbon nanotubes, J. Membr. Sci. 493 (2015) 224–231.
[27] X. Song, J. Gao, N. Zheng, H. Zhou, Y.-W. Mai, Interlaminar toughening in carbon fiber/epoxy composites interleaved with CNT-decorated polycaprolactone nanofibers, Composites Communications 24 (2021) 100622.
[28] Y.Q. Liu, Z.L. Yao, A. Adronov, Functionalization of single-walled carbon nanotubes with well-defined polymers by radical coupling, Macromolecules 38 (2005) 1172–1179.
[29] J.H. Zou, S.I. Khondaker, Q. Huo, L. Zhai, A general strategy to disperse and functionalize carbon nanotubes using conjugated block copolymers, Adv. Funct. Mater. 19 (2009) 479–483.
[30] M. Qiu, B. Zhang, H. Wu, L. Cao, X. He, Y. Li, J. Li, M. Xu, Z. Jiang, Preparation of anion exchange membrane with enhanced conductivity and alkaline stability by incorporating ionic liquid modified carbon nanotubes, J. Membr. Sci. 573 (2019) 1–10.
[31] K.-K. Yan, L. Jiao, S. Lin, X. Ji, Y. Lu, L. Zhang, Superhydrophobic electrospun nanofiber membrane coated by carbon nanotubes network for membrane distillation, Desalination 437 (2018) 26–33.
[32] X. Yao, J. Li, L. Kong, Y. Wang, Surface functionalization of carbon nanotubes by direct encapsulation with varying dosages of amphiphilic block copolymers, Nanotechnology 26 (2015) 325601.
[33] P.S. Goh, A.F. Ismail, S.M. Sanip, B.C. Ng, M. Aziz, Recent advances of inorganic fillers in mixed matrix membrane for gas separation, Separ. Purif. Technol. 81 (2011) 243–264.
[34] S.M. Park, J. Jung, S. Lee, Y. Baek, J. Yoon, D.K. Seo, Y.H. Kim, Fouling and rejection behavior of carbon nanotube membranes, Desalination 343 (2014) 180–186.
[35] G. Liu, Y. Xu, Y.D. Han, J.B.A. Wu, J.L. Xu, H. Meng, X. Zhang, Immobilization of lysozyme proteins on a hierarchical zeolitic imidazolate framework (ZIF-8), Dalton Trans. 46 (2017) 2114–2121.
[36] D. Venturoli, B. Rippe, Ficoll and dextran vs. globular proteins as probes for testing glomerular permselectivity: effects of molecular size, shape, charge, and deformability, Am. J. Physiol. Ren. Physiol. 288 (2005) 605–613.
[37] Q. Lan, C. Feng, K. Ou, Z. Wang, Y. Wang, T. Liu, Phenolic membranes with tunable sub-10-nm pores for nanofiltration and tight-ultrafiltration, J. Membr. Sci. 640 (2021) 119858.